scientific reports

Check for updates

OPEN

Suppressing spectator-induced dephasing through optimized dynamical decoupling implementation

Hayoung Jeong[1], Youngdu Kim[2], Beomgyu Choi[2], Minkyun Cho[1], Seungwook Woo[2], Yonuk Chong[2]✉, Yong-Ho Lee[1] & Hwan-Seop Yeo[1]✉

Dynamical decoupling (DD) is a well-established technique for protecting quantum systems from environmental noise. DD effectively mitigates decoherence in superconducting quantum computing systems, where precise implementation plays a crucial role in optimizing its performance. This study investigates how DD implementation timing and sequence design critically affect spectator-induced dephasing from adjacent qubits. We find that excited states of adjacent qubits dramatically degrade operational qubit coherence. We demonstrate that DD sequences applied to adjacent qubits effectively suppress this dephasing. This protection persists even when adjacent qubits remain in superposition states during the sequence. Through systematic characterization of Carr-Purcell-Meiboom-Gill (CPMG) sequences, we show that implementation timing strongly impacts protection effectiveness. While optimal timing achieves substantial coherence enhancement, improper sequence delays can severely degrade protection. Our results highlight the importance of precise timing control for implementing DD in optimizing multi-qubit quantum circuits.

In superconducting quantum computing systems, maintaining coherence across multiple coupled qubits presents unique challenges due to inter-qubit interactions and environmental noise[1–3]. Fixed-frequency transmon architectures exhibit inherent ZZ coupling between neighboring qubits (typically 40–100 kHz) and crosstalk between control lines[4,5], leading to coherent phase errors that scale with qubit count. During idle periods, qubits show increased error rates from adjacent two-qubit operations, significantly impacting circuit fidelity[6]. Dynamical decoupling (DD) sequences have proven effective at suppressing environmental noise in various quantum platforms, from trapped ions to superconducting circuits[7–12]. DD offers a hardware-efficient approach that can be implemented during idle times in quantum circuits without requiring additional physical resources, making it valuable for larger quantum computing systems. While DD seems to be a practical method, precise implementation methodology should be investigated in optimizing its performance in multi-qubit architectures.

DD sequences, in convention, decouple qubits from environmental noise by applying precisely designed pulses to average out unwanted interactions[13,14]. Recent studies have demonstrated DD effectiveness beyond simple decoherence suppression, achieving significant improvements in quantum algorithm execution fidelity and enabling extended coherence times in error correction protocols[15,16].

However, current multi-qubit systems face significant implementation challenges. The limited operational parallelism in quantum circuits creates unavoidable idle times, while variable gate latencies (ranging from 20 ns for single-qubit to 300 ns for two-qubit gates) and data movement requirements further complicate DD timing[6,17]. Traditional DD protocols, typically applied to operational qubits, do not fully address the combined effects of crosstalk and decoherence in fixed-frequency transmon architectures. These challenges raise questions about optimal DD sequence design, particularly regarding sequence implementation timing in the presence of spectator qubits.

Among various DD techniques, Carr-Purcell-Meiboom-Gill (CPMG) sequences are well-known for mitigating dephasing caused by noise sources in quantum systems[18–20]. These sequences are implemented by applying a series of π-pulses to the qubit, where "CPMG-N" refers to applying N total π-pulses. CPMG sequences are widely used in quantum computing, particularly in superconducting qubits, to suppress low-frequency noise by decoupling qubits from undesired effects[12,21,22]. Recent studies have demonstrated that

[1]Korea Research Institute of Standards and Science (KRISS), 267 Gajeong-ro, Yuseong-gu, Daejeon 34113, Republic of Korea. [2]SKKU Advanced Institute of Nano Technology(SAINT), Sungkyunkwan University, Suwon 16419, Republic of Korea. ✉email: yonuk@skku.edu; repia9909@gmail.com

CPMG and implementing syncopated DD can effectively cancel ZZ interactions between qubits, making it particularly valuable for mitigating crosstalk in multi-qubit system[23,24]. However, while the previous work has explored relative timing shifts between pulses[24], further case studies examining sequence delay as a distinct parameter across various CPMG orders are needed. Such studies are essential for understanding how DD can be properly applied in multi-qubit systems, as real-world implementations cannot always maintain precisely synchronized timing ratios.

In this study, we investigate how DD implementation timing and sequence design affect both operational and adjacent qubit coherence through detailed characterization of sequence parameters. By applying DD sequences to adjacent qubits rather than operational qubits, we provide effective protection against state-decay-induced dephasing originating from ZZ interactions. This approach maintains its effectiveness even when adjacent qubits remain in superposition states during the sequence - a critical capability for practical quantum circuits. Through systematic study of CPMG sequences, we investigate the relationship between timing parameters and protection effectiveness. Optimal timing achieves substantial coherence enhancement. However, improper sequence delays can reduce protection effectiveness dramatically. These findings provide practical guidelines for implementing DD protection in multi-qubit quantum circuits and establish a framework for optimizing coherence protection in increasingly complex quantum systems.

Results

Adjacent Qubit-Induced decoherence in multi-qubit systems

We utilize three fixed-frequency transmon qubits in a row, coupled by a fixed frequency resonator, as shown in Fig. 1. Qubit 2(Q2) is defined as an operational qubit, located in the middle of the qubit chain. The adjacent qubits (Q1, Q3) act as noise sources through their ZZ interactions with Q2. This configuration allows us to systematically study how adjacent qubit states affect operational qubit coherence and evaluate the DD effectiveness.

To evaluate the impact of adjacent qubit states on operational qubit coherence, we analyzed protection effects on adjacent qubits using a normalized performance ratio (p). This metric is defined as the ratio of measured coherence time to a reference value of 27.35 μs - the baseline T_2 of operational qubit Q2 when adjacent qubits are in their ground state. This normalization enables direct comparison of coherence degradation or enhancement across different configurations and operating conditions.

Impact of adjacent qubit population on operational qubit coherence

We characterized Q2's coherence by varying the excited state population of adjacent qubits Q1 and Q3 using scaled π-pulses (Fig. 2). The scaling factor s controls the amplitude of the π-pulse, where $s = 0$ leaves the qubit in ground state and $s = 1$ implements a full π-pulse for complete excitation. Starting from $s = 0$, where Q2 exhibits

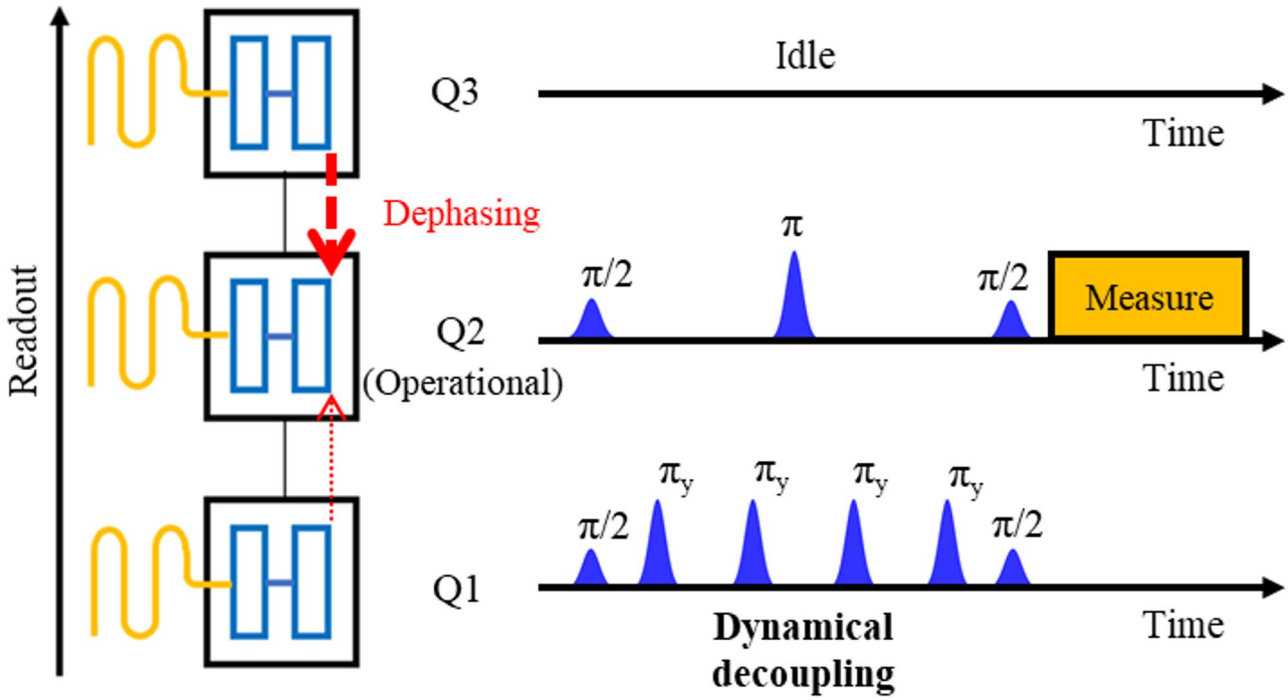

Fig. 1. Schematic of DD implementation in a three-qubit system. A linear array of three coupled transmon qubits where the central qubit (Q2) serves as the operational qubit while adjacent qubits (Q1, Q3) act as noise sources through ZZ coupling. Red arrows indicate dephasing induced by adjacent qubits, which is suppressed when CPMG sequences are applied. This DD implementation protects Q2's coherence by mitigating crosstalk effects from neighboring qubits.

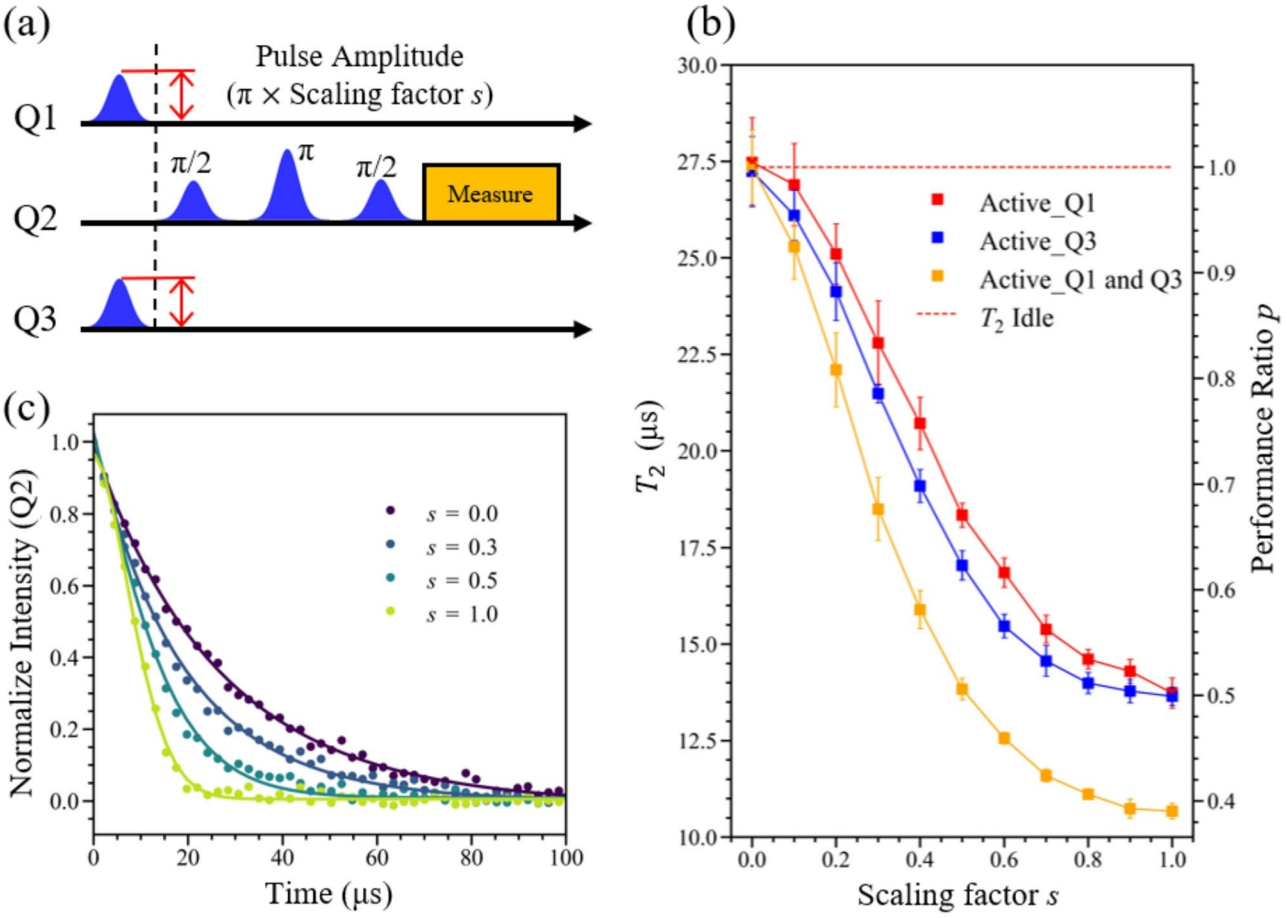

Fig. 2. Coherence degradation of operational qubit Q2 due to adjacent qubit excitation. (**a**) Pulse sequences showing Hahn echo measurement of Q2's coherence time (T_2) while scaled π-pulses are applied to adjacent qubits Q1 and Q3. (**b**) Q2's average T_2 and normalized performance ratio versus π-pulse scaling, measured for three cases: excitation of Q1 only, Q3 only, and simultaneous excitation of both Q1 and Q3. (c) Resulting T_2 decay curves of Q2 showing coherence dependence on the excitation of adjacent qubits (both Q1 and Q3 active).

$T_2 = 27.35$ μs ($p = 1$), we observed continuous degradation in coherence as s increased. Individual excitation of either Q1 or Q3 reduced the performance ratio to approximately 0.5, corresponding to $T_2 \approx 13.7$ μs in both cases. This symmetric response might be aligned with the similar ZZ coupling strengths (46 kHz for Q2-Q1 and 40 kHz for Q2-Q3) and relaxation times (T_1 of 19.7 μs for Q1 and 15.5 μs for Q3).

Due to ZZ interactions, the operational qubit experiences state-dependent frequency shifts based on adjacent qubit states[4,25]. When an excited adjacent qubit spontaneously decays to its ground state, this induces an abrupt phase change in the operational qubit. Given the finite lifetime of real qubits, this state-decay-induced dephasing becomes challenging whenever adjacent qubits are populated. Our observations show this effect becomes particularly pronounced with simultaneous excitation of both adjacent qubits, where p drops below 0.4. While the ZZ interaction itself is coherent, the random timing of decay events introduces incoherent noise contributions that sum independently[26,27]. The relationship between dephasing magnitude, qubit lifetime, and ZZ coupling strength presents an interesting avenue for theoretical investigation, though detailed modeling remains a task for future work.

We observed a continuous decrease in the performance ratio even with partial excitation ($0 < s < 1$) of adjacent qubits, with particular significance at $s = 0.5$ - equivalent to placing adjacent qubits in superposition states. This state represents the condition encountered during CPMG sequence implementation, making our findings directly relevant to DD protection strategies. The smooth degradation in p contrasts with earlier models that considered only discrete ground/excited state effects[28], establishing the importance of intermediate population states in multi-qubit systems. While a complete theoretical treatment of arbitrary quantum states remains an open challenge, our experimental results motivate the investigation of DD sequence optimization for protecting against dephasing when adjacent qubits occupy superposition states. We address this aspect in the following sections through systematic characterization of DD performance.

Mitigation of adjacent qubit-induced dephasing by implementing DD sequence

Having established the impact of state-decay-induced dephasing from adjacent qubits, we next investigated dephasing mitigation via dynamical decoupling. We measured the pure dephasing time (T_2^*) of the operational qubit while applying CPMG sequences to the adjacent qubits. To ensure consistent timing control, we matched the total duration of both Ramsey and CPMG sequences (Fig. 3). Our investigation began with a Hahn echo sequence applied to the adjacent qubit, representing the simplest form of DD[29,30]. While less effective than CPMG for noise reduction, this approach provided a baseline for observing Ramsey oscillations of the operational qubit and determining its T_2^* through fitting.

We then increased the number of π-pulses in the CPMG sequence to evaluate its impact on the operational qubit's performance ratio p. Figure 3 shows the improvement in p of the operational qubit Q2 for both

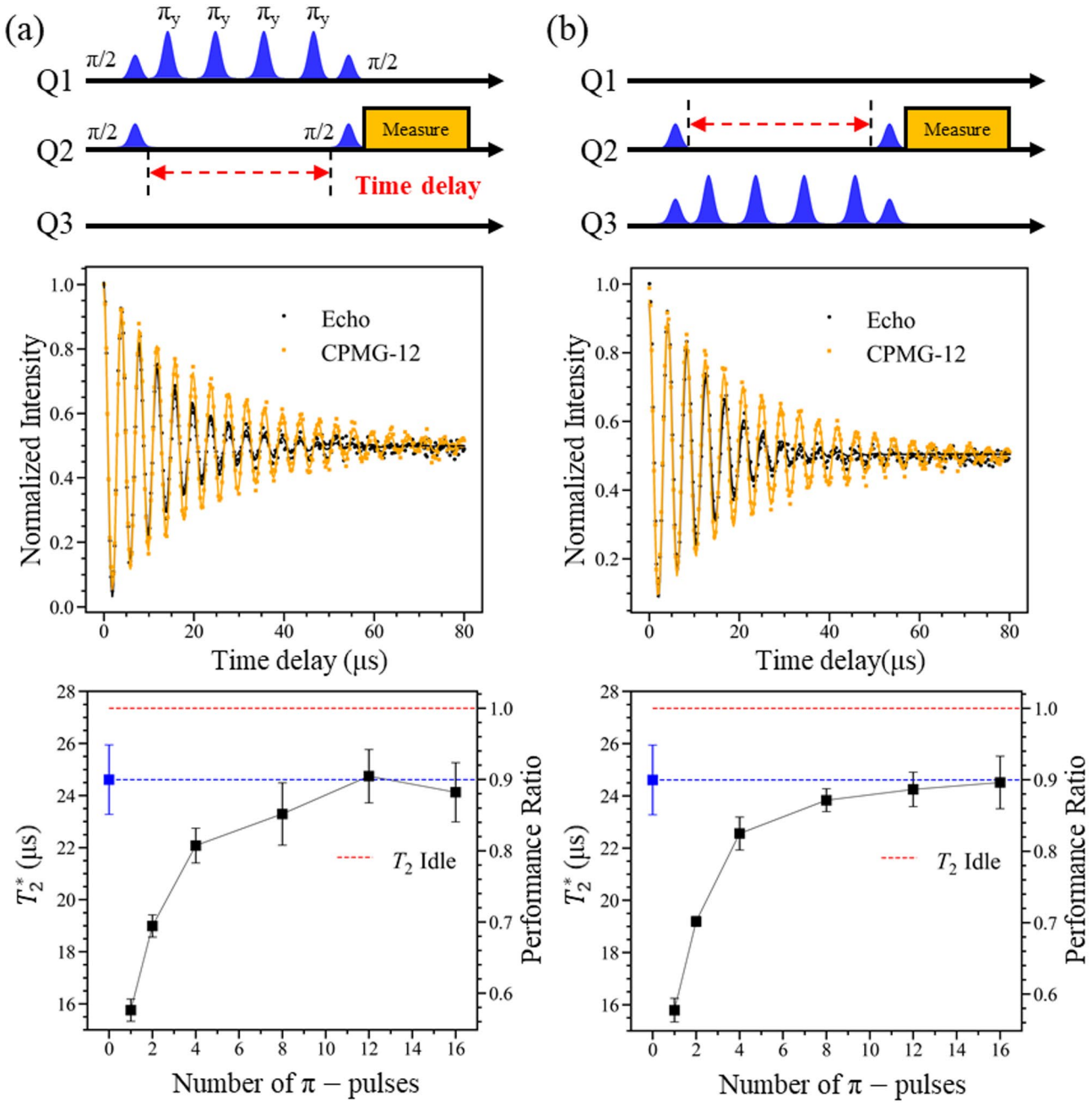

Fig. 3. Measurement of operational qubit Q2's pure dephasing time (T_2^*) under adjacent qubit dynamical decoupling and Hahn Echo. (**a**, **b**) Pulse sequence diagrams showing Ramsey measurements on Q2 while CPMG sequences are applied to either adjacent qubit Q1 or Q3. The total duration of Ramsey and CPMG sequences are matched to ensure synchronized start and end times. Plots show Q2's average T_2^* versus number of π-pulses in the CPMG sequence. Blue dashed lines indicate T_2^* values measured with adjacent qubits in their idle.

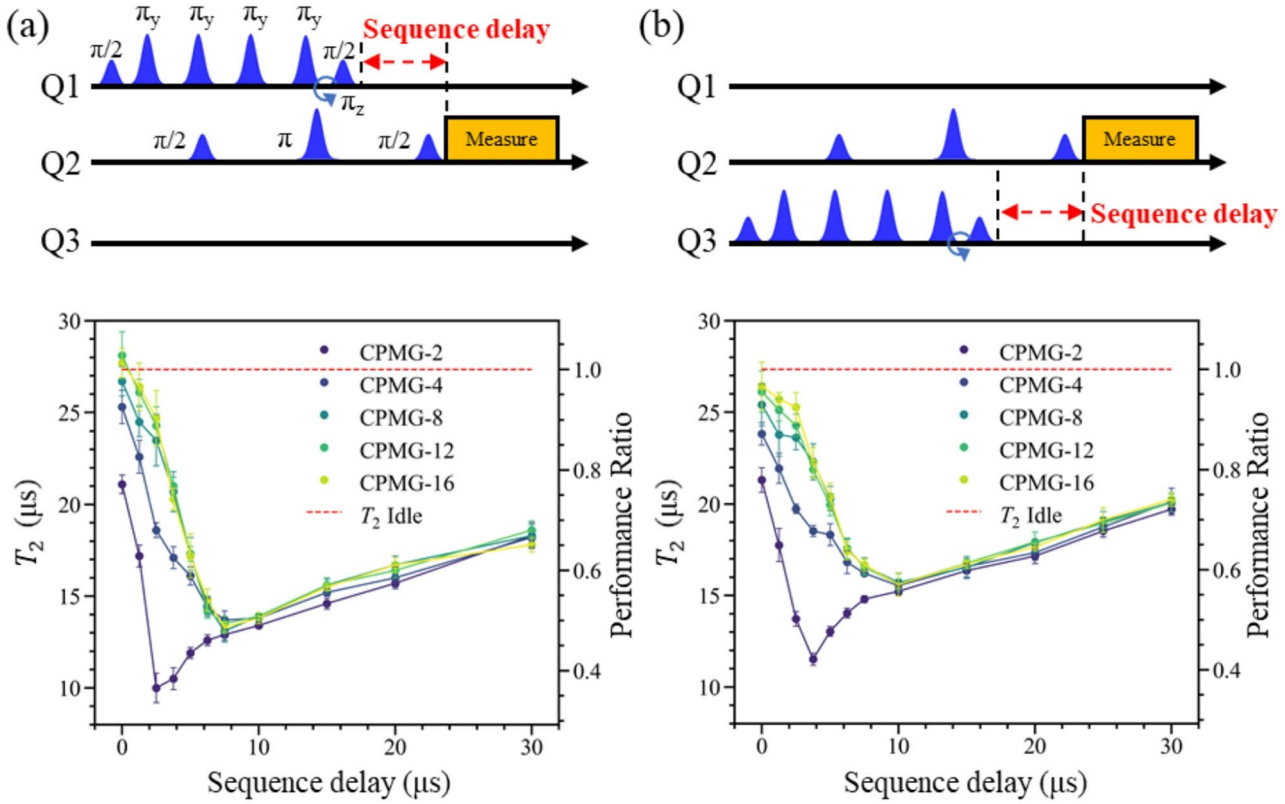

Fig. 4. Impact of DD sequence timing on operational qubit coherence. (a, b) Pulse sequences showing Q2's coherence time (T_2) measurement using Hahn echo while CPMG sequences with varying delays are applied to either adjacent qubit Q1 or Q3. A virtual-Z gate with π-phase was applied to bring the adjacent qubit back to the ground state. Plots show Q2's T_2 with normalized performance ratio versus sequence delay from CPMG-2 to CPMG-16. Red dashed lines indicate Q2's T_2 with idle adjacent qubits. These results show that while higher CPMG orders recover spectator-induced dephasing at zero sequence delay, even small sequence delays significantly reduce this protective effect, highlighting the importance of proper implementation timing.

configurations. In the Q2-Q1 configuration, p increased from 0.57 with a single π-pulse to 0.90 with 12 π-pulses. Similarly, the Q2-Q3 configuration exhibited enhancement from 0.58 to 0.89 when implementing 16 π-pulses. As the number of π-pulses increased, p approached the reference value observed when adjacent qubits were in their idle (indicated by blue dashed line in Fig. 3).

DD is well-known to effectively suppressing both coherent and incoherent sources of decoherence. The coherent errors arise from residual ZZ interactions and subsequent state-decay-induced dephasing[31,32], while incoherent errors stem from environmental fluctuations including charge noise and magnetic field fluctuations[33,34]. Our earlier result demonstrated that adjacent qubits in superposition states degrade the operational qubit coherence. Notably, DD sequences improve the coherence while adjacent qubits remain in superposition states during the sequence. This indicates that there was a successful suppression of decay-induced dephasing effects.

The observed increase in p with higher π-pulse counts implies that DD sequences successfully decouple low-frequency errors. However, the upper bound of p reaches only 0.90 when adjacent qubits are in their idle, rather than approaching unity achieved with an echo-sequence T_2 on the operational qubit alone. In ideal conditions, we would expect p to approach identity[35], but our results show that intrinsic noise components affecting the operational qubit persist even with optimal DD implementation on adjacent qubits. While DD effectively decouples the operational qubit from adjacent qubit noise, it does not directly shield the operational qubit from environmental decoherence. This observation highlights that DD sequences on adjacent qubits specifically target crosstalk-induced decoherence while leaving other decoherence channels unaffected.

Coherence time of operational qubit by implementing DD sequence on adjacent qubits

We investigated the impact of DD timing on the operational qubit's T_2 with varying sequence delays and CPMG orders. The measurement protocol employed a Hahn echo sequence on the operational qubit concurrent with CPMG sequence on adjacent qubits. We maintained equal total duration for both Hahn echo and CPMG sequences. A virtual-Z gate with π-phase was applied before the final π/2 pulse to bring the adjacent qubit back to the ground state after the DD sequence.

Figure 4 shows the T_2 and the performance ratio of the operational qubit as a function of sequence delay. With zero sequence delay, T_2 of the operational qubit increased with the number of π-pulses in both the Q2-

Q1 and Q2-Q3 configurations. The coherence time reached the values comparable to those observed with idle adjacent qubits (red dashed line in Fig. 4) when applying up to 16 π-pulses.

Interestingly, a few μs of delay dramatically reduces T_2 of the operational qubit. With CPMG-2, a delay of 2.5 μs caused T_2 to drop to 9.9 μs in the Q2-Q1 configuration, yielding a performance ratio of 0.36. The Q2-Q3 configuration showed similar degradation, with the performance ratio falling to 0.42 at 3.75 μs delay. This is significantly less than 0.5 when Q3 is in a fully excited state, as compared to the values in Fig. 2. For sequences beyond CPMG-2, both configurations exhibited a performance ratio around 0.5 and 0.57 for a 10 μs sequence delay. These values approach the performance ratio of 0.5 observed under individual excitation of adjacent qubits at a maximum scaling factor *s*.

Within the sequence delay range of 0 to 7.5 μs, increasing the number of π-pulses partially compensated for timing misalignment. This deterioration in coherence occurred regardless of CPMG order. These results indicate that improper implementation of DD is highly detrimental to the coherence of the operational qubit. In other words, it is crucial that the proper implementation of DD sequence to keep coherence in complex quantum circuits.

We observed an unexpected behavior at longer sequence delays. The reduction in T_2 began to reverse when delays exceeded approximately 10 μs, with coherence times gradually increasing at longer delays. At delays beyond 80 μs (not shown), T_2 recovered to the upper bound observed with idle adjacent qubits. This recovery suggests a transition to a regime where the sequences operate independently, effectively decoupling their mutual influence. This observation provides insight into the timescales over which DD sequences maintain their coherent interaction effects.

We also applied DD to both adjacent qubits (Q1 and Q3) simultaneously (not shown) at zero sequence delay, and observed that the T_2 of Q2 increased with the number of π-pulses in the CPMG sequences, reaching a saturated value similar to that observed when the adjacent qubits were in their idle. Based on this observation, we expect similar overall trends when applying sequence delays to both adjacent qubits as shown in Fig. 4. However, the detailed trend of T_2 as a function of sequence delay may differ due to the additive nature of crosstalk effects from both adjacent qubits, which depends on their respective T_1, T_2, and ZZ coupling strengths. Further study with various qubit combinations is necessary to fully characterize these combined effects.

Furthermore, as the coherence time of the operational qubit improved with DD applied to the adjacent qubits, we also examined the behavior of the adjacent qubits using the same sequences shown in Fig. 4, with 0 sequence delay. As the number of π-pulses in the CPMG sequence increased, the T_2 of the adjacent qubits improved, ultimately saturating to the T_2 value observed when the operational qubit was in the idle (as detailed in the Supplementary Information). These findings demonstrate that our DD approach effectively enhances the coherence of both the operational and adjacent qubit.

Discussion

Our investigation reveals that spectator qubit decay significantly impacts operational qubit coherence in a superconducting quantum system, quantitatively demonstrated through consistent performance ratio analysis. When multiple adjacent qubits are excited, the coherence performance ratio drops below 0.4, yet optimal DD implementation can restore it to 0.9. This metric enables direct comparison across different system configurations and protection strategies.

The effectiveness of DD protection critically depends on implementation timing. Timing alignment emerges as the most critical parameter - even microsecond-scale misalignment between DD and measurement sequences significantly degrades protection. Notably, the protection persists even with spectator qubits in superposition states - a crucial capability for practical quantum computing where qubits commonly exist in superposition during algorithm execution[36]. We believe our DD approach can be effectively extended to multi-qubit entangled states, as demonstrated in previous works, where DD was shown to mitigate crosstalk and preserve coherence even in entangled systems[6,15,37]. While DD effectively suppresses crosstalk-induced decoherence, it leaves other environmental channels unaffected, suggesting opportunities for complementary protection strategies.

These findings provide insights for a proper way of implementing DD in multi-qubit circuits, though theoretical aspects remain to be fully explored. Future work matching experimental data with comprehensive models incorporating ZZ coupling strengths and qubit lifetimes would enhance our understanding of protection limits. Additionally, investigating the integration of timing-optimized DD with other error mitigation techniques could lead to more robust protection schemes.

Methods

Commercial dilution refrigerator (BlueFors LD400) was utilized to cool the superconducting qubit chip to a base temperature of approximately 10 mK. Fixed-frequency transmon qubits were selected for their well-characterized coherence properties and stable operation. Qubit control were performed individually and measured by multiplexed readout with Zurich Instruments SHFQC. The drive pulses for all three qubits were Gaussian-shaped with a duration of 64 ns. The readout pulses were Gaussian square-shaped and had a duration of 1.5 μs. To protect the qubits from external decoherence, cryogenic filtering with low-pass and infrared filters was used. Isolators prevented back-action and reflections in the RF lines, ensuring clean readout signals. Readout amplification was achieved using HEMTs at 4 K as low-temperature amplifiers.

Data availability

The datasets used and/or analyzed during the current study are available from the corresponding author on reasonable request.

Received: 4 December 2024; Accepted: 13 May 2025
Published online: 28 May 2025

References

1. Zeissler, K. Superconducting qubits at scale. *Nat. Electron.* **1**, 1 (2024).
2. Bravyi, S. et al. The future of quantum computing with superconducting qubits. *J. Appl. Phys.* **132**, 160901 (2022).
3. Schlör, S. et al. Correlating decoherence in Transmon qubits: Low frequency noise by single fluctuators. *Phys. Rev. Lett.* **123**, 190502 (2019).
4. Kandala, A. et al. Demonstration of a high-fidelity CNOT gate for fixed-frequency transmons with engineered ZZ suppression. *Phys. Rev. Lett.* **127**, 130501 (2021).
5. Zhao, P. et al. High-contrast ZZ interaction using superconducting qubits with opposite-sign anharmonicity. *Phys. Rev. Lett.* **125**, 200503 (2020).
6. Das, P. et al. Adapt: Mitigating idling errors in qubits via adaptive dynamical decoupling. *MICRO-54: 54th Annual IEEE/ACM International Symposium on Microarchitecture* (2021).
7. Arrazola, I. et al. Pulsed dynamical decoupling for fast and robust two-qubit gates on trapped ions. *Phys. Rev. A*. **97**, 052312 (2018).
8. Pham, L. M. et al. Enhanced solid-state multispin metrology using dynamical decoupling. *Phys. Rev. B*. **86**, 045214 (2012).
9. Bar-Gill, N. et al. Solid-state electronic spin coherence time approaching one second. *Nat. Commun.* **4**, 1743 (2013).
10. Sukachev, D. D. et al. Silicon-vacancy spin qubit in diamond: a quantum memory exceeding 10 Ms with single-shot state readout. *Phys. Rev. Lett.* **119**, 223602 (2017).
11. Nadj-Perge, S. et al. Spin–orbit qubit in a semiconductor nanowire. *Nature* **468**, 7327 (2010).
12. Bylander, J. et al. Noise spectroscopy through dynamical decoupling with a superconducting flux qubit. *Nat. Phys.* **7**, 565–570 (2011).
13. Viola, L. et al. Dynamical decoupling of open quantum systems. *Phys. Rev. Lett.* **82**, 2417 (1999).
14. Khodjasteh, K. et al. Fault-tolerant quantum dynamical decoupling. *Phys. Rev. Lett.* **95**, 180501 (2005).
15. Tripathi, V. et al. Suppression of crosstalk in superconducting qubits using dynamical decoupling. *Phys. Rev. Appl.* **18**, 024068 (2022).
16. Pokharel, B. et al. Demonstration of fidelity improvement using dynamical decoupling with superconducting qubits. *Phys. Rev. Lett.* **121**, 220502 (2018).
17. Khadirsharbiyani, S. et al. Minimizing coherence errors via dynamic decoupling. In Proceedings of the 38th ACM International Conference on Supercomputing, 164–175 (2024).
18. Schenken, W. K. et al. Long-lived coherences in strongly interacting spin ensembles. *Phys. Rev. A*. **110**, 032612 (2024).
19. Janitz, E., Bhaskar, M. K. & Childress, L. Cavity quantum electrodynamics with color centers in diamond. *Optica* **7**, 1232–1252 (2020).
20. Medford, J. et al. Scaling of dynamical decoupling for spin qubits. *Phys. Rev. Lett.* **108**, 086802 (2012).
21. Han, J. et al. Characterizing noise correlation and enhancing coherence via qubit motion. *Fund Res.* **1**, 10–15 (2021).
22. Cywiński, Ł. et al. How to enhance dephasing time in superconducting qubits. *Phys. Rev. B*. **77**, 174509 (2008).
23. Ezzell, N. et al. Dynamical decoupling for superconducting qubits: a performance survey. *Phys. Rev. Appl.* **20**, 064027 (2023).
24. Evert, B. et al. Syncopated dynamical decoupling for suppressing crosstalk in quantum circuits. arXiv:2403.07836 (2024).
25. Watanabe, S. et al. ZZ-interaction-free single-qubit-gate optimization in superconducting qubits. *Phys. Rev. A*. **109**, 012616 (2024).
26. Young, K. C. et al. Qubits as spectrometers of dephasing noise. *Phys. Rev. A*. **86**, 012314 (2012).
27. Hahn, T. et al. Influence of excited state decay and dephasing on phonon quantum state Preparation. *Phys. Rev. B*. **100**, 024306 (2019).
28. Jurcevic, P. & Govia, L. C. G. Effective qubit dephasing induced by spectator-qubit relaxation. *Quantum Sci. Technol.* **7**, 045033 (2022).
29. Meiboom, S. et al. Modified spin-echo method for measuring nuclear relaxation times. *Rev. Sci. Instrum.* **29**, 688–691 (1958).
30. Bar-Gill, N. et al. Suppression of spin-bath dynamics for improved coherence of multi-spin-qubit systems. *Nat. Commun.* **3**, 858 (2012).
31. Mundada, P. et al. Suppression of qubit crosstalk in a tunable coupling superconducting circuit. *Phys. Rev. Appl.* **12**, 054023 (2019).
32. Ni, Z. et al. Scalable method for eliminating residual ZZ interaction between superconducting qubits. *Phys. Rev. Lett.* **129**, 040502 (2022).
33. Rower, D. A. et al. Evolution of 1/f flux noise in superconducting qubits with weak magnetic fields. *Phys. Rev. Lett.* **130**, 220602 (2023).
34. Wilen, C. D. et al. Correlated charge noise and relaxation errors in superconducting qubits. *Nature* **594**, 369–373 (2021).
35. Ahmad, H. G. et al. Investigating the individual performances of coupled superconducting Transmon qubits. *Condens. Matter*. **8**, 29 (2023).
36. Krantz, P. et al. A quantum Engineer's guide to superconducting qubits. *Appl. Phys. Rev.* **6**, 021318 (2019).
37. Kim, Y. et al. Scalable error mitigation for noisy quantum circuits produces competitive expectation values. *Nat. Phys.* **19.5**, 752–759 (2023).

Acknowledgements

This work was supported by the National Research Foundation of Korea (NRF) grant funded by the Korea government (MSIT) (2022M3K2A1083855, 2022M3K4A1097631, 2022M3K2A1084250, 2020M3H3A1110365). This research was supported by the Development of Quantum-Based Measurement Technologies funded by the Korea Research Institute of Standards and Science (KRISS-2024-GP2024-0013).

Author contributions

H.J. and H.-S.Y. designed the concept of experiments. Y.K. and B.C. designed and fabricated superconducting qubits. H.J. conducted all the experiments. M.C established experimental setup. M.C and S.W. contributed discussion on implementing dynamic decoupling scheme. Y.C. and Y.-H.L. contributed discussions on the experimental results. H.J. and H.-S.Y. wrote the manuscript. All authors discussed the results and commented on the manuscript.

Declarations

Competing interests

The authors declare no competing interests.

Additional information

Supplementary Information The online version contains supplementary material available at https://doi.org/10.1038/s41598-025-02370-8.

Correspondence and requests for materials should be addressed to Y.C. or H.-S.Y.

Reprints and permissions information is available at www.nature.com/reprints.

Publisher's note Springer Nature remains neutral with regard to jurisdictional claims in published maps and institutional affiliations.